Available online at www.sciencedirect.com
SCIENCE DIRECT®

Journal of Volcanology and Geothermal Research 122 (2003) 221–242

Journal of volcanology and geothermal research

www.elsevier.com/locate/jvolgeores

# Exploration and discovery in Yellowstone Lake: results from high-resolution sonar imaging, seismic reflection profiling, and submersible studies

L.A. Morgan [a,*], W.C. Shanks III [a], D.A. Lovalvo [b], S.Y. Johnson [a], W.J. Stephenson [a], K.L. Pierce [c], S.S. Harlan [d], C.A. Finn [a], G. Lee [a], M. Webring [a], B. Schulze [e], J. Dühn [e], R. Sweeney [a], L. Balistrieri [f]

[a] *U.S. Geological Survey, Denver Federal Center, P.O. Box 25046, MS 966, Denver, CO 80225-0046, USA*
[b] *Eastern Oceanics, 25 Limekiln Rd., West Redding, CT 06896, USA*
[c] *U.S. Geological Survey, Northern Rocky Mountain Science Center, P.O. Box 173492, Montana State University, Bozeman, MT 59717-3492, USA*
[d] *George Mason University, Department of Geography and Earth Science, Fairfax, VA 22030-4444, USA*
[e] *L-3 Communication Elac Nautik GmbH Neufeldtstrasse, D-24118 Kiel, Germany*
[f] *U.S. Geological Survey, University of Washington, School of Oceanography, P.O. Box 55351, Seattle, WA 98195-5351, USA*

Received 10 June 2002; accepted 22 November 2002

'No portion of the American continent is perhaps so rich in wonders as the Yellow Stone'
(F.V. Hayden, September 2, 1874)

**Abstract**

Discoveries from multi-beam sonar mapping and seismic reflection surveys of the northern, central, and West Thumb basins of Yellowstone Lake provide new insight into the extent of post-collapse volcanism and active hydrothermal processes occurring in a large lake environment above a large magma chamber. Yellowstone Lake has an irregular bottom covered with dozens of features directly related to hydrothermal, tectonic, volcanic, and sedimentary processes. Detailed bathymetric, seismic reflection, and magnetic evidence reveals that rhyolitic lava flows underlie much of Yellowstone Lake and exert fundamental control on lake bathymetry and localization of hydrothermal activity. Many previously unknown features have been identified and include over 250 hydrothermal vents, several very large (> 500 m diameter) hydrothermal explosion craters, many small hydrothermal vent craters (~1–200 m diameter), domed lacustrine sediments related to hydrothermal activity, elongate fissures cutting post-glacial sediments, siliceous hydrothermal spire structures, sublacustrine landslide deposits, submerged former shorelines, and a recently active graben. Sampling and observations with a submersible remotely operated vehicle confirm and extend our understanding of the identified features. Faults, fissures, hydrothermally inflated domal structures, hydrothermal explosion craters, and sublacustrine landslides constitute potentially significant geologic hazards. Toxic elements derived from hydrothermal processes also may significantly affect the Yellowstone ecosystem. Published by Elsevier Science B.V.

* Corresponding author. Tel.: +1-303-273-8646; Fax: +1-303-273-8600. *E-mail address:* lmorgan@usgs.gov (L.A. Morgan).

0377-0273/03/$ – see front matter Published by Elsevier Science B.V.
doi:10.1016/S0377-0273(02)00503-6

*Keywords:* Yellowstone Lake; Yellowstone caldera; hydrothermal explosion craters; rhyolitic lava flows; hydrothermal vents; swath bathymetry; sub-bottom seismic reflection profiling; submersible remotely operated vehicle; siliceous spires; domed lacustrine sediments; fissures; submerged shorelines; caldera resurgence; sublacustrine landslide deposits; fluid flow

## 1. Introduction

Powerful geologic processes in Yellowstone National Park have contributed to the unusual shape of Yellowstone Lake, which straddles the southeast margin of the Yellowstone caldera (Fig. 1), one of the world's largest active silicic volcanoes. Volcanic forces contributing to the lake's form include the explosive caldera-forming 2.05-Ma eruption of the Huckleberry Ridge Tuff followed by eruption of the 0.64-Ma Lava Creek Tuff to form the Yellowstone caldera (Christiansen, 1984, 2001; Hildreth et al., 1984; U.S.G.S., 1972). Following explosive, pyroclastic-dominated activity, large-volume rhyolitic lava flows were emplaced along the caldera margin, infilling much of the caldera (Fig. 1A,B). A smaller caldera-forming event about 140 ka, comparable in size to Crater Lake, OR, USA, created the West Thumb basin (Christiansen, 1984; U.S.G.S., 1972). Several significant glacial advances and recessions continued to shape the lake and overlapped the volcanic events (Pierce, 1974, 1979; Richmond, 1976, 1977). Glacial scour deepened the central basin of the lake and the faulted South and Southeast Arms (Fig. 1B). More recent dynamic processes shaping Yellowstone Lake include currently active fault systems, development of a series of post-glacial shoreline terraces, and post-glacial (~12–15 ka) hydrothermal explosion events, which created the Mary Bay crater complex and other craters.

Formation of hydrothermal features in Yellowstone Lake is related to convective meteoric hydrothermal fluid circulation, steam separation during fluid ascent, and possible $CO_2$ accumulation and release above an actively degassing magma chamber. Hydrothermal explosions result from accumulation and release of steam and/or $CO_2$, possibly reflecting changes in confining pressure that accompany and may accelerate failure and fragmentation of overlying lithologies. Sealing of surficial discharge conduits due to hydrothermal mineral precipitation contributes to overpressuring and catastrophic failure. Heat flow maps show that both the northern and West Thumb basins of Yellowstone Lake have an extremely high heat flux (1650–15 600 mW/m$^3$) compared to other areas in the lake (Morgan et al., 1977). Earthquake epicenter locations indicate that the area north of the lake is seismically active (Smith, 1991), and remotely operated vehicle (ROV) studies identify hydrothermally active areas within the lake (Balistrieri et al., 2003; Klump et al., 1988; Remsen, 1990; Shanks et al., 2003).

The objective of the present work is to understand the geologic processes that shape the lake floor. Our three-pronged approach to mapping the floor of Yellowstone Lake located, imaged, and sampled bottom features such as sublacustrine hot-spring vents and fluids, hydrothermal deposits, hydrothermal explosion craters, rock outcrops, slump blocks, faults, fissures, and submerged shorelines. Chemical studies of the vents indicate that ~10% of the total deep thermal water flux in Yellowstone National Park occurs on the lake bottom. Hydrothermal fluids containing potentially toxic elements (As, Sb, Hg, Mo, W, and Tl) significantly influence lake chemistry and possibly the lake ecosystem (Balistrieri et al., 2003). ROV observations indicate that shallow hydrothermal vents are home to abundant bacteria and amphipods that form the base of the food chain. This food chain includes indigenous cutthroat trout and piscivorous exotic lake trout, as well as grizzly bears, bald eagles, and otters that feed on the potamodromous cutthroat trout during spawning in streams around the lake (Chaffee et al., 2003). Finally, our results document and identify potential geologic hazards associated with sublacustrine hydrothermal explosions, landslides, faults, and fissures in Yellowstone National Park.

## 2. Methods

Surveys of Yellowstone Lake between 1999 and 2001 utilized state-of-the-art bathymetric, seismic, and submersible ROV equipment. The multi-beam swath-bathymetric surveys employed a Sea-Beam 1180 (180 kHz) instrument with a depth resolution of $\leq 1\%$ water depth. Water depth varied from $\sim 4$ to 133 m in the survey areas. The multi-beam instrument uses 126 beams arrayed over a 150° ensonification angle to map a swath width of 7.4 times water depth. Sub-bottom seismic reflection profiling utilized an EdgeTech SB-216S, which sweeps a frequency range from 2 to 10 kHz and has a beam angle of 15–20°. Both the swath unit transducer and the sub-bottom unit were rigidly mounted to the transom of an 8-m aluminum boat used for survey purposes. The new survey, which was navigated to an accuracy of $\leq 1$ m using differential GPS, utilized over 122 000 000 soundings to produce high-resolution continuous overlapping coverage of the lake's bathymetry. Simultaneously, we surveyed over 2500 linear km with high-resolution seismic reflection profiling that penetrated the upper $\sim 25$ m of the lake bottom.

The Eastern Oceanics submersible ROV is small ($\sim 1.5$ m $\times$ 1 m $\times$ 1 m) and attached to the vessel with a 200-m tether. The ROV provides live videographic coverage and remote control of cameras and sampling equipment. The ROV has a full-depth rating of 300 m and is capable of measuring temperature, conductivity, and depth, and of retrieving hydrothermal vent water samples and rock samples up to 40 cm long.

## 3. Results and discoveries of high-resolution mapping

### *3.1. Topographic margin of the caldera*

Geologic maps (U.S.G.S., 1972; Christiansen, 2001; Richmond, 1974) show the topographic margin of the Yellowstone caldera is below lake level in Yellowstone Lake between the western entrance to Flat Mountain Arm and north of Lake Butte (Fig. 1B). Our mapping of the central basin of Yellowstone Lake in 2001 identified the topographic margin of the 0.64-Ma Yellowstone caldera as a series of elongated troughs northeast from Frank Island across the deep basin of the lake. Based on our new data and high-resolution aeromagnetic data (Finn and Morgan, 2002), we infer the topographic margin of the Yellowstone caldera to pass through the southern part of Frank Island.

East and north of Frank Island, the topographic margin of the caldera follows a series of discontinuous moderate amplitude magnetic lows in the reduced-to-pole magnetic map (Finn and Morgan, 2002) (Fig. 1C). The anomalies coincide with bathymetric troughs (Fig. 2A,D) identified by the new mapping. The location of the caldera west of Frank Island continues through a series of subtle bathymetric lows toward the head of Flat Mountain Arm. Here, the caldera margin separates Tertiary andesitic rocks and pre-caldera and caldera-forming rhyolitic ignimbrites to the south from young, post-collapse rhyolitic lava flows to the north and northwest (U.S.G.S., 1972).

Pronounced magnetic highs over much of the Absaroka Range along the eastern side of Yellowstone Lake (Fig. 1C) are related to rugged topographic relief and highly magnetized Tertiary andesitic debris flows, dikes, and lava flows. Similar magnetic anomalies over The Promontory, which separates South Arm from Southeast Arm (Figs. 1B and 2A), are associated with Tertiary andesitic lava and debris flows prominently exposed in cliffs several hundred meters high. The same magnetic signature occurs along the eastern shore of the lake north and slightly west of Park Point where a thin exposure of the Lava Creek Tuff overlies the magnetically dominant Tertiary volcanic rocks. North and east of Plover Point in southern Yellowstone Lake, the magnetic signature is similar to that of nearby Tertiary volcanic rocks; we suggest Tertiary volcanic rocks are present at depth and are overlain by younger Yellowstone Group volcanic rocks (Figs. 1C and 2A). These positive magnetic anomalies are caused by Tertiary volcanic rocks at the surface, as exposed at The Promontory and in the Absaroka Range, or alternatively, are buried at shallow depths in the

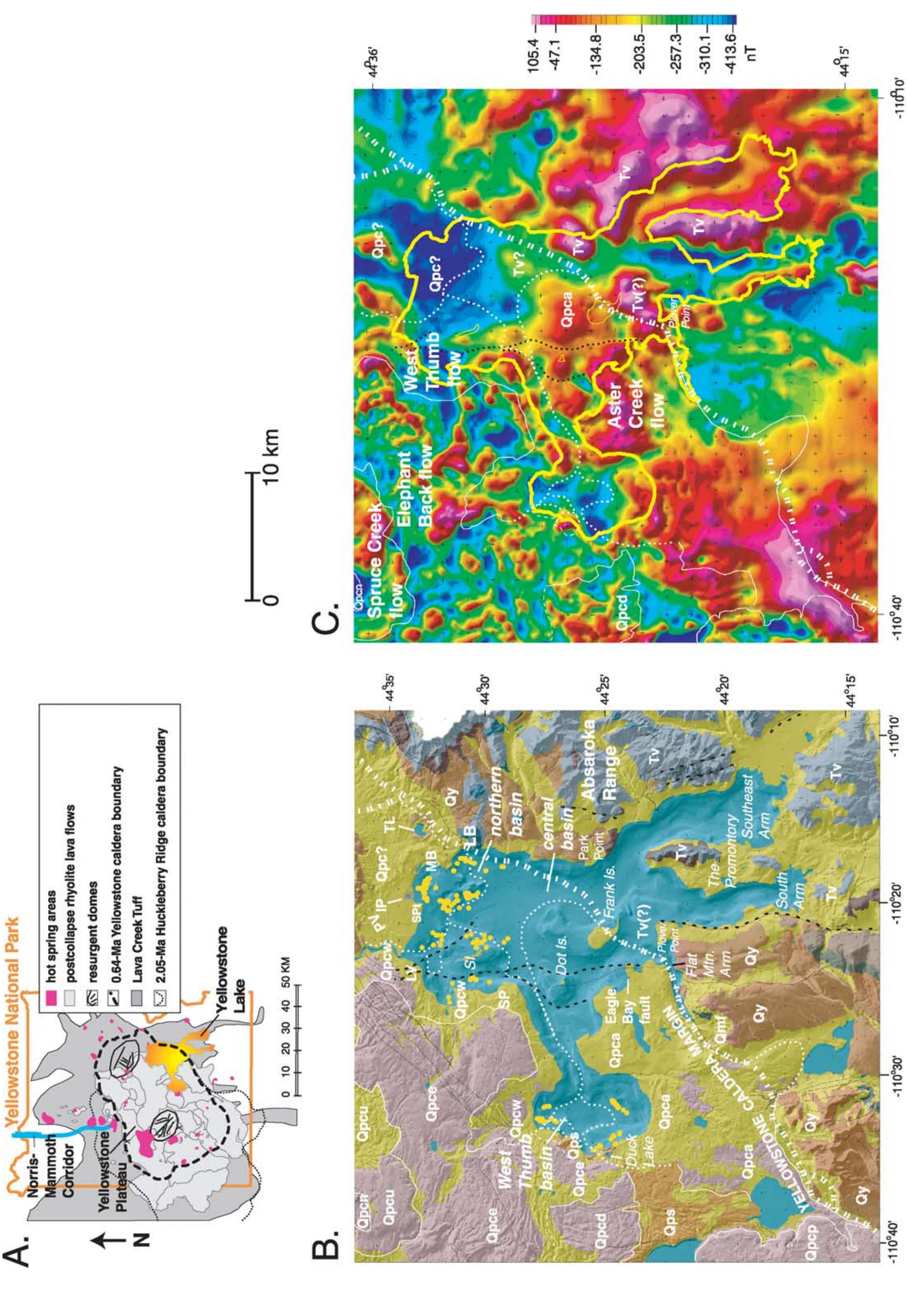
A.
B.
C.
Yellowstone National Park
Norris-Mammoth Corridor
Yellowstone Plateau
Yellowstone Lake
N
hot spring areas
postcollapse rhyolite lava flows
resurgent domes
0.64-Ma Yellowstone caldera boundary
Lava Creek Tuff
2.05-Ma Huckleberry Ridge caldera boundary
0 10 20 30 40 50 KM
West Thumb basin
Duck Lake
Eagle Bay fault
Dot Is.
Frank Is.
Plover Point
Flat Mtn. Arm
The Promontory
Southeast Arm
South Arm
northern basin
central basin
Park Point
Absaroka Range
YELLOWSTONE CALDERA MARGIN
Spruce Creek flow
Elephant Back flow
West Thumb flow
Aster Creek flow
0 10 km
105.4
-47.1
-134.8
-203.5
-257.3
-310.1
-413.6
nT
-110°40'
-110°30'
-110°20'
-110°10'
44°35'
44°30'
44°25'
44°20'
44°15'
44°36'

lake, such as north of Plover Point extending northward into the southern third of Frank Island (Finn and Morgan, 2002). The high amplitude of the magnetic anomaly over the southern part of Frank Island is comparable to that present in the Absaroka Mountains immediately to the east or on The Promontory, suggesting a similar Tertiary source.

In contrast, the moderate amplitudes of positive magnetic anomalies in the reduced-to-the-pole map over the northern part of Frank Island are similar to those associated with post-collapse rhyolitic lava flows, such as seen in much of the West Thumb, Hayden Valley, and Aster Creek flows (Fig. 1B,C; Finn and Morgan, 2002). The topographic margin of the caldera immediately south of Frank Island may be represented by a series of concentric zones, possibly related to down-dropped blocks on the topographic margin of the caldera margin (Fig. 2D). These areas may contain significant amounts of Tertiary volcanic rocks as part of the slumped caldera wall, contributing to the magnetic signature seen in the reduced-to-the-pole aeromagnetic map of the southern third of Frank Island (Fig. 1C).

Another possible slumped wall of the caldera may be due west of Elk Point (Fig. 2D) where bathymetric mapping shows a slab-like structure rising 40 m from the lake floor. The reduced-to-the-pole magnetic map (Finn and Morgan, 2002) shows a moderate amplitude anomaly associated with this structure, different in its signature than that described for the majority of Tertiary volcanic rocks in the area. Perhaps this structure is a slumped and rotated block of Tertiary volcanic material. Alternatively, this structure may be a northeastward extension of a thin section of the post-collapse caldera rhyolitic Aster Creek flow that has been separated from the main unit by glacial scouring. The thickest ice cap in the most recent glacial period resided in the central basin of Yellowstone Lake (Pierce, 1979). Additional areas of northeast-trending glacial scour can be seen immediately west of the deep central basin and continuing south onto land in the Delusion Lake area between West Thumb basin and Flat Mountain Arm (Fig. 2D).

### 3.2. Rhyolitic lava flows

Large-volume subaerial rhyolitic lava flows (10's of km$^3$) on the Yellowstone Plateau control much of the local topography and hydrology. Characteristic lava flow morphologies include near-vertical margins (some as high as 700 m), rubbly flow carapaces, hummocky or ridged tops, and strongly jointed interiors. Stream drainages tend to occur along flow boundaries, rather than within flow interiors. Many flows have vitro-

Fig. 1. (A) Index map showing the 0.64-Ma Yellowstone caldera, the distribution of its erupted ignimbrite (the Lava Creek Tuff), post-caldera rhyolitic lava flows, subaerial hydrothermal areas, and the two resurgent domes. The inferred margin of the 2.05-Ma Huckleberry Ridge caldera is also shown. Data are from Christiansen (2001). (B) Geologic shaded relief map of the area surrounding Yellowstone Lake in Yellowstone National Park. Geologic mapping is from U.S.G.S. (1972) and Yellowstone Lake bathymetry is from previous bathymetric mapping of the lake that employed a single-channel echo sounder (Kaplinski, 1991). Yellow markers in West Thumb basin and the northern basin are locations of hydrothermal vents mapped by seismic reflection and multi-beam sonar. The lithologic symbols are as follows: Tv: Tertiary volcanic rocks; Qmf: Flat Mountain flow; Qps: tuff of Bluff Point; Qpcd: Dry Creek flow; Qpcm: Mary Lake flow; Qpca: Aster Creek flow; Qpcw: West Thumb flow; Qpce: Elephant Back flow; Qpcu: Spruce Creek flow; Qpcn: Nez Perce flow; Qpcp: Pitchstone Plateau flow; Qs: Quaternary sediments (yellow); Qy: Quaternary Yellowstone Group ignimbrites (Christiansen, 2001; U.S.G.S., 1972). General location of Yellowstone caldera margin (bold white dashed line) is from Christiansen (1984), with modifications from Finn and Morgan (2002). White lines: lava flow margins; black lines: faults or fissures. IP: Indian Pond; LB: Lake Butte; LV: Lake Village; MB: Mary Bay; PV: Pelican Valley; SI: Stevenson Island; SP: Sand Point; SPt: Storm Point; TL: Turbid Lake. (C) Color-shaded relief image of high-resolution, reduced-to-the-pole aeromagnetic map (Finn and Morgan, 2002). Sources of the magnetic anomalies are shallow and include the post-caldera rhyolite lava flows (some outlined in white), which have partly filled in the Yellowstone caldera. Commonly, rhyolitic lava flow margins have impermeable glassy rinds that are not subject to hydrothermal alteration, producing distinctive positive magnetic anomalies. Extensive areas of negative magnetic anomalies in the West Thumb and northern basins and along the caldera margin northeast of the lake are areas of high heat flow and intense present and past hydrothermal alteration as suggested by sublacustrine vent locations (Figs. 1B and 5D). Qpca: Aster Creek flow; Tv: Tertiary volcanic rocks.

A.

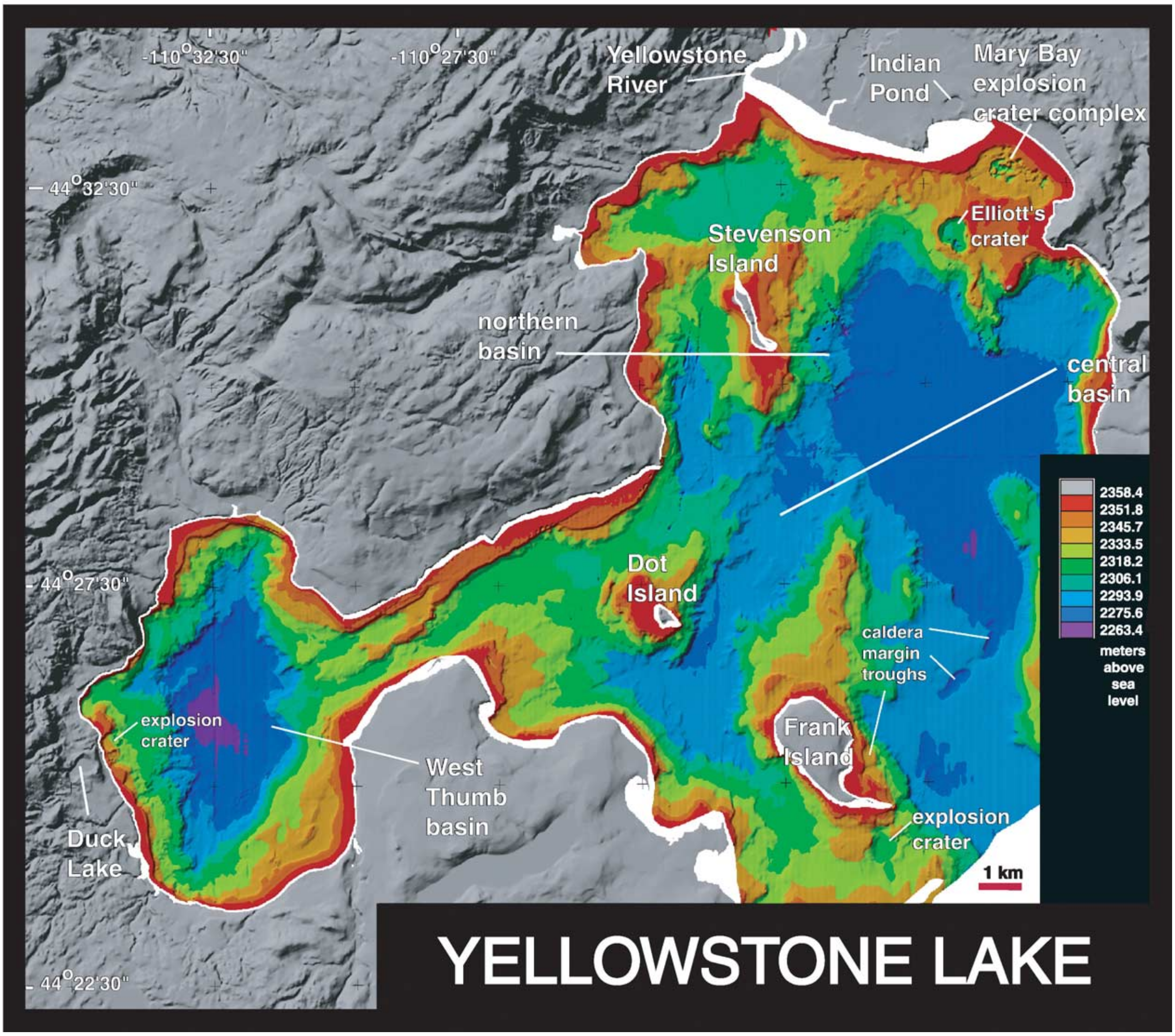


Fig. 2. (A) High-resolution color-shaded relief bathymetric map of the West Thumb, northern, and central basins of Yellowstone Lake, acquired by multi-beam sonar imaging and seismic reflection mapping from 1999 to 2001, is shown merged with the shaded relief topographic map of the area around Yellowstone Lake. This map shows previously unknown features such as rhyolitic lava flows that underlie post-glacial sediments, several large (> 500 m wide) hydrothermal explosion craters, numerous hydrothermal vents, fissures west of Stevenson Island and extending into the central basin, submerged lakeshore terraces, and landslide deposits along the eastern margin of the lake near the caldera margin. In the central basin, the bathymetric margin of the Yellowstone caldera is marked by a series of elongate troughs. (B) New high-resolution bathymetric map of the West Thumb basin of Yellowstone Lake, acquired by multi-beam sonar imaging and seismic mapping in 2000, showing a previously unknown ~500-m-wide hydrothermal explosion crater (east of Duck Lake), numerous hydrothermal vents, submerged lakeshore terraces, and inferred rhyolitic lava flows that underlie 7–10 m of post-glacial sediments (see Fig. 1B for geologic unit acronyms). (C) High-resolution bathymetric map of the northern basin of Yellowstone Lake, acquired in 1999, showing large hydrothermal explosion craters in Mary Bay and south-southeast of Storm Point, numerous smaller craters related to hydrothermal vents, and landslide deposits along the eastern margin of the lake near the caldera margin (Fig. 1). Post-caldera rhyolitic lava flows underlie much of the northern basin (see Fig. 1B for geologic unit acronyms). Fissures west of Stevenson Island and the graben north of it may be related to the young Eagle Bay fault (see Fig. 1B). (D) High-resolution bathymetric map of the central lake basin, acquired by multi-beam sonar imaging and seismic mapping in 2001, showing the Yellowstone caldera topographic margin, a large hydrothermal explosion crater south of Frank Island, and numerous faults, fissures, and hydrothermal vents as indicated (see Fig. 1B for geologic unit acronyms).

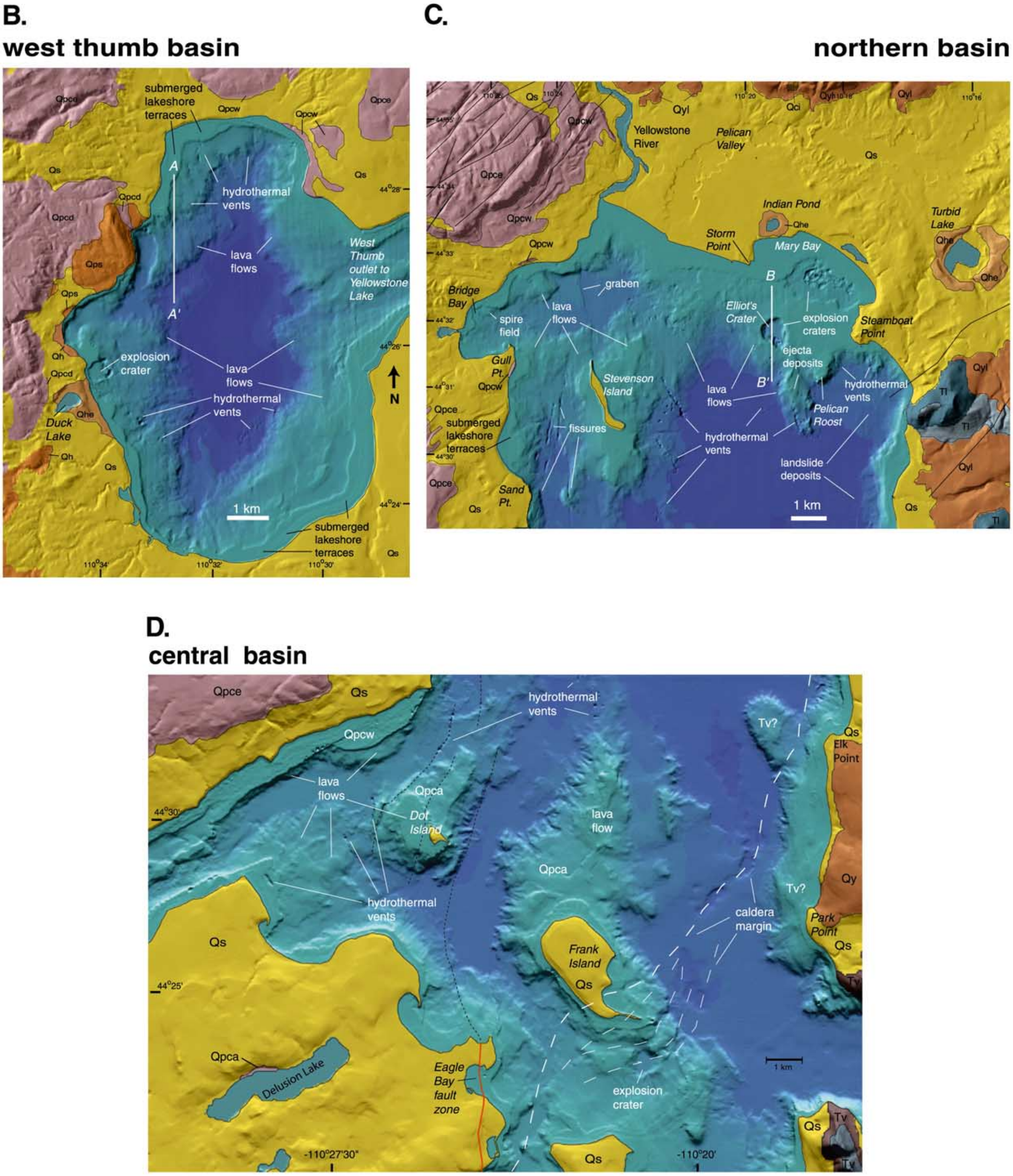


Fig. 2 (*Continued*).

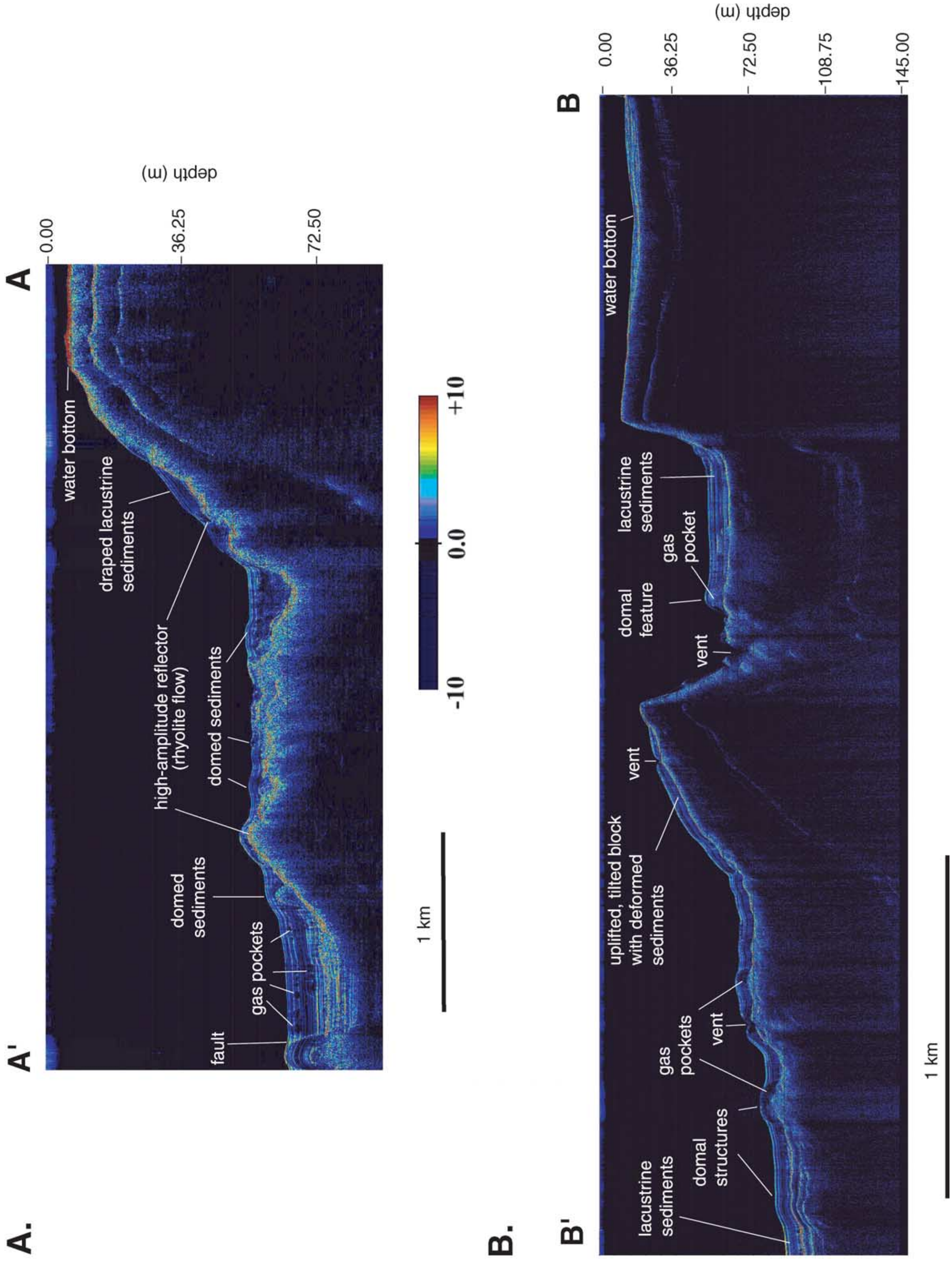
A.
A
A'
depth (m)
0.00
36.25
72.50
water bottom
draped lacustrine sediments
high-amplitude reflector (rhyolite flow)
domed sediments
domed sediments
gas pockets
fault
1 km
+10
0.0
-10
B.
B
B'
depth (m)
0.00
36.25
72.50
-108.75
-145.00
water bottom
lacustrine sediments
gas pocket
domal feature
vent
vent
uplifted, tilted block with deformed sediments
vent
gas pockets
domal structures
lacustrine sediments
1 km

phyric exterior rinds with shrinkage cracks and sheet-jointed crystallized interior zones. Spherulitic and lithophysal zones commonly include large cavities. Breccias occur locally.

A major discovery of the lake surveys is the presence of previously unrecognized rhyolitic lava flows underlying much of the lake floor. We believe the lava flows are key to controlling many morphologic and hydrothermal features in the lake.

Areas of the lake bottom around the perimeter of West Thumb basin (Fig. 2A,B) have steep, nearly vertical margins, bulbous edges, and irregular hummocky surfaces, similar to post-collapse rhyolitic lava flows of the Yellowstone Plateau. Seismic reflection profiles in the near-shore areas of West Thumb basin show high-amplitude reflectors beneath about 7–10 m of layered lacustrine sediments (Fig. 3A). We interpret these sublacustrine features to be sediment-veneered rhyolitic lava flows that partly fill the interior of the 140-ka West Thumb caldera.

Based on air-gun seismic reflection data, Otis et al. (1977) recognized a high-amplitude reflector at various depths beneath glaciolacustrine sediments in the lake; despite the hummocky top to the reflector and the extensive exposures of post-collapse rhyolitic lava flows to the west and northwest of Yellowstone Lake, however, the reflector was misidentified as the Lava Creek Tuff. Whereas the Lava Creek Tuff and the post-collapse lava flows are both high-silica rhyolites, many of their physical properties differ, such as cooling zonation patterns and magnetic characteristics, and these differences have significant implications for localization of hydrothermal activity.

Unaltered, topographically high post-collapse rhyolite flow deposits produce moderate amplitude positive magnetic anomalies. Magnetic lows over these flows are related to topographically low basins and faults as well as hydrothermally altered areas (Finn and Morgan, 2002). In contrast to the rhyolite flows, the wide range of bulk susceptibility values precludes clear identification of the Lava Creek Tuff as an individual geologic unit on the high-resolution aeromagnetic map. Positive anomalies are observed over the most magnetic and thickest (50–100 m) sections of the ignimbrite in elevated terrain (Finn and Morgan, 2002).

Areas such as the West Thumb and Potts geyser basins in West Thumb basin, and Mary Bay in the northern basin, currently have extremely high heat flow values (1650–15 600 mW/m$^2$; Morgan et al., 1977), high enough to contribute significantly to the demagnetization of the rocks present by hydrothermal alteration. Current heat flow values in Bridge Bay (580 mW/m$^2$; Morgan et al., 1977) in the northern basin are relatively low compared to Mary Bay yet the Bridge Bay area has low magnetic intensity values in the reduced-to-the-pole magnetic map (Finn and Morgan, 2002); evidence for past hydrothermal activity is present as inactive hydrothermal vents and structures and may have been responsible for demagnetization of the rocks there. Additionally, south of Bridge Bay and west of Stevenson Island, low magnetic intensity values reflect active hydrothermal venting and relatively high heat flow values (Morgan et al., 1977). Low magnetic intensity values in the northern West Thumb basin may be also due to past hydrothermal activity, as evidenced by vent structures there. Field examination of rhyolite flows shows that many areas with low magnetic intensity values correspond to areas with hydrothermal activity or faulting or fracturing along which hy-

Fig. 3. (A) High-resolution seismic reflection image from northwestern West Thumb basin (section A–A′, Fig. 2B) showing high-amplitude (red) reflector interpreted as a sub-bottom rhyolitic lava flow. Glacial and lacustrine sediments, marked in blue, overlie this unit. The data amplitudes have been debiased and spatially equalized only. No additional gain corrections or filtering are applied. (B) High-resolution seismic reflection image (section B–B′, Fig. 2C) across part of Elliott's explosion crater. This shows small vents, gas pockets, and domed sediments in the lacustrine sediments that overlie the crater flank. Lacustrine sediment thickness in the main crater indicates 8–13 thousand years of deposition since the main explosion. More recent explosions in the southern part of the large crater ejected post-crater lacustrine sediments and created new, smaller craters. Colors are the same as Fig. 3A.

drothermal alteration has occurred. In contrast, the mapped extent of the Lava Creek Tuff is not revealed in the magnetic data. This difference may be due in part to the quenched vertical and thick (> 100 m) flow margins common in many of the large-volume rhyolitic lava flows whereas the Lava Creek Tuff is more tabular in extent, is generally thinner, and does not have quenched edges.

Because of the high-resolution, shallow-penetration seismic reflection method we employed, rhyolitic lava flow tops are imaged as high-amplitude reflectors only in areas where sediment cover is thin. In other areas, high-resolution aeromagnetic data provide critical evidence. Comparison of geologic maps (Fig. 1B) (Blank, 1974; Christiansen, 1974; Christiansen and Blank, 1975; Richmond, 1973) with the high-resolution aeromagnetic maps (Finn and Morgan, 2002) shows a crude relation of magnetic anomalies to the mapped individual lava flows on land (Fig. 1C). The magnetic signatures, combined with the high-resolution bathymetric and seismic reflection data, allow identification and correlation of sediment-covered rhyolitic lava flows far out into the lake (Figs. 1 and 2). For example, the Aster Creek flow (Qpca) southwest of the lake (Fig. 1C) is associated with a consistent moderately positive magnetic anomaly that extends over the lake in the southeast quadrant of West Thumb basin, along the southern half of the West Thumb channelway, and over the central basin of the lake well past Dot and Frank Islands (Figs. 1 and 2). The Aster Creek flow has few mapped faults and few areas that have been hydrothermally altered. Similarly, the West Thumb flow (Qpcw) can be traced into the lake in northeastern West Thumb basin, along the northern half of West Thumb channelway, and into the northern basin beneath Stevenson Island and Bridge Bay (Fig. 2c). In contrast, the Elephant Back flow contains a well-developed system of northeast-trending faults or fissures that has been extensively altered so that the magnetic signature of this unit is fractured with a wide range of values in magnetic intensity (Fig. 2D).

In the northern basin, rhyolitic lava flows are inferred mainly from the bathymetry. Interpretation of the magnetic data is somewhat more complicated owing to high temperatures and extensive hydrothermal alteration reflected in the low values of magnetic intensity. Extremely high heat flow in the Mary Bay area (1650–15 600 mW/m$^2$) (Morgan et al., 1977) and abundant sublacustrine hydrothermal activity (Fig. 1B) have resulted in hydrothermal alteration destroying or significantly reducing the magnetic susceptibility of minerals in rocks and sediments producing the observed negative magnetic anomalies.

A rhyolitic body present at depth in the northern basin and lower Pelican Valley (Fig. 2C) is indicated from hydrothermally altered quartz-bearing felsite lithic clasts present in the hydrothermal explosion breccia of Mary Bay and prevalent in the alluvium of the lower Pelican Valley (Qpc?, Fig. 1B). This unit has not been described before and is not mapped. We suggest the felsite clasts are derived from either a buried volcanic or shallow intrusive unit beneath the lower Pelican Valley and the northern lake basin. This felsite produces the moderate positive magnetic anomaly seen in the reduced-to-the-pole map (Qpc?, Fig. 1C) in the lower Pelican Valley (Finn and Morgan, 2002).

Topographically low areas and hydrothermally altered areas cause magnetic lows over the Yellowstone Lake area. The altered portions of lava flows often produce characteristic high-amplitude (200–600 nT) circular or oval, magnetic lows, particularly evident over the active geyser basins. Modeling of two of the characteristic anomalies within the caldera shows that the lows are caused by the magnetization contrast between ~200 and 500 m thick non-magnetic altered zones and adjacent rhyolites with magnetizations between 3 and 6 A/m (Finn and Morgan, 2002). Hydrothermal explosion craters would be expected to produce magnetic lows due to topography as well as hydrothermal alteration.

Field examination of subaerial rhyolitic lava flows indicates that negative magnetic anomalies, for the most part, are associated with extensive hydrothermal alteration or, in places, alteration due to emplacement of lava flows into water, such as ancestral Yellowstone Lake. For example, the West Thumb rhyolite flow due west of the

Yellowstone River is glassy, flow-banded, and fresh; the magnetic intensity values in this area generally are high (Figs. 1B,C and 2C). In contrast, in areas where flows were emplaced into water, such as the West Thumb rhyolite flow exposed on the northeast shore of West Thumb basin (Figs. 1B and 2B), magnetic intensity values are low (Fig. 1C). The low magnetic values of flows emplaced into water may be primarily carried by the fine-grained and altered matrix in the massive rhyolitic breccias, highly fractured perlitic vitrophyre, clastic dikes, and entrained stream, beach, and lake sediments in an altered matrix.

### 3.3. Large hydrothermal explosion craters

Subaerial hydrothermal explosions have occurred repeatedly over the past 12 ka in Yellowstone National Park (Muffler et al., 1971) and are confined primarily within the boundaries of the Yellowstone caldera (Fig. 1). Large (> 500 m) circular, steep-walled, flat-bottomed depressions are mapped at several sites in Yellowstone Lake in the West Thumb, central, and northern basins (Fig. 2). These are interpreted as large composite hydrothermal explosion craters similar in origin to those on land, such as Duck Lake, Pocket Basin, the 8.3-ka Turbid Lake crater, and the 3.0-ka Indian Pond crater (Figs. 1B and 2B,C) (Morgan et al., 1998; Pierce et al., 2002; Muffler et al., 1971).

A newly discovered 500-m diameter sublacustrine explosion crater in the western part of West Thumb basin near the currently active West Thumb geyser basin is only 300 m northeast of Duck Lake (Fig. 2A,B), a post-glacial (< 12 ka) hydrothermal explosion crater (Muffler et al., 1971; Christiansen, 1974, 2001; Richmond, 1973; U.S.G.S., 1972). Here, heat flow values are as high as 1500 mW/m$^2$ (Morgan et al., 1977), reflecting the hydrothermal activity that contributed to the formation of the offshore explosion crater. The 500-m-wide West Thumb explosion crater is surrounded by 12–20-m-high nearly vertical walls and has several smaller nested craters along its eastern edge. These nested craters are as deep as 40 m and are younger than the main crater. Temperatures of hydrothermal fluids emanating from the smaller northeast nested crater have been measured at 72°C by ROV.

Another newly discovered large subaqueous hydrothermal explosion crater is the > 600-m-wide elongate, steep-walled, flat-floored crater south of Frank Island (Fig. 2D). Muted topography suggests that this explosion crater is one of the oldest still recognizable in Yellowstone Lake. Further, this crater occurs in an area where heat flow values are at present relatively low. Submersible investigations do not indicate hydrothermal activity within the crater.

In the northern basin of Yellowstone Lake, Mary Bay contains a roughly 1-km by 2-km area of coalesced explosion craters (Morgan et al., 1998; Wold et al., 1977) (Fig. 2A,C), thus making it the world's largest known hydrothermal explosion system (Browne and Lawless, 2001). Boiling temperature in the deep part of Mary Bay is about 160°C. Submersible investigations show that fluids from a 35-m-deep hydrothermal vent in Mary Bay have temperatures near the 120°C limit of the temperature probes used, reflecting extremely high heat flow values in this area (Morgan et al., 1977). Radiocarbon dates from charcoal in breccia deposits and underlying soils exposed in the wave-cut cliffs along the shore of Mary Bay indicate that eruption of this crater occurred at 13.4 ka (Morgan et al., 1998; Pierce et al., 2002). Detailed stratigraphic measurements of the breccia deposit indicate that multiple explosions and emplacements occurred during formation of this large and complex feature. A clean, planar-bedded sand overlying varved lake sediments occurs as a sedimentary interbed between breccia deposits within the Mary Bay breccia deposit; the fine sand unit may represent deposition from a wave-generated event associated with the development of the Mary Bay complex (Morgan et al., 1998, 2002).

One kilometer southwest of the Mary Bay crater complex is another newly discovered large (~800 m diameter) composite depression informally referred to as Elliott's Crater (Fig. 2C), named after Henry Elliott who helped map Yellowstone Lake in the 1871 Hayden survey (Mer-

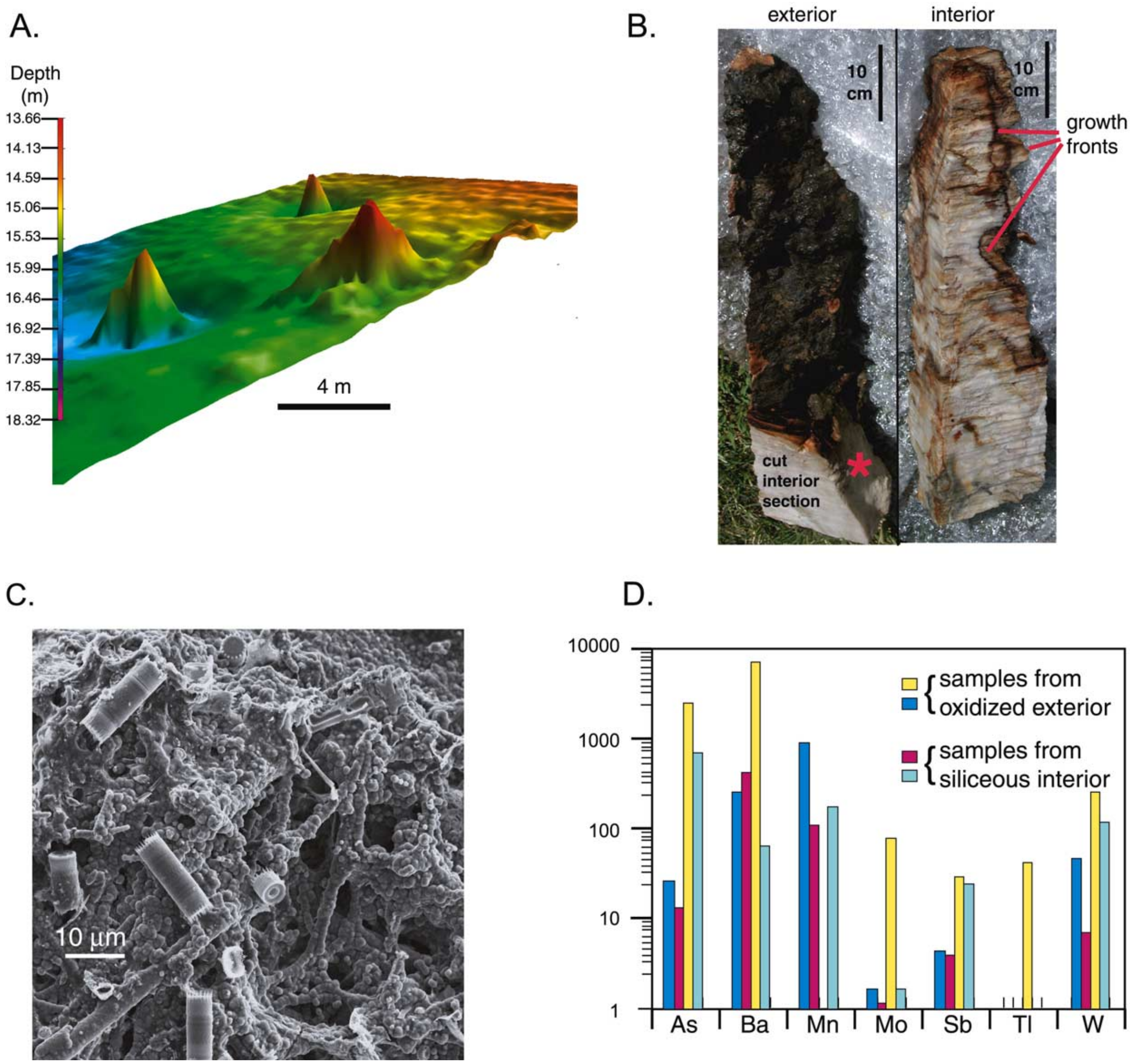


Fig. 4. (A) Bathymetric image of spires in Bridge Bay, showing their roughly conical shapes. About a dozen such siliceous sinter spires occur near Bridge Bay, some as tall as 8 m. Many of the spires occupy lake-bottom depressions (possible former explosion or collapse craters). (B) Photographs of the exterior and interior of a 1.4-m-tall spire sample recovered from Bridge Bay by National Park Service divers. The sediment–water interface of this spire is apparent near the base of the exterior section as seen in the dramatic contrast in color from the outer rind of red-brown ferromanganese oxide to the light gray below the sediment–water interface (red asterisk). Former growth fronts on the spire can be seen on the interior section. (C) SEM image of diatoms, silicified filamentous bacteria, and amorphous silica from a spire sample. (D) Summary bar graph of chemical composition of spire samples showing substantial concentrations of arsenic, barium, manganese, molybdenum, antimony, thallium, and tungsten.

rill, 1999). Development of Elliott's hydrothermal explosion crater is best illustrated in a north–south seismic reflection profile (Fig. 3B). Zones of non-reflectivity in the seismic profile on the floor and flanks of the large crater probably represent hydrothermally altered and possibly heterolithic explosion breccia deposits, similar in character to those exposed on land and associated with subaerial explosion craters (Muffler et al., 1971). Seismic profiles in the hummocky area southeast of Elliott's Crater also are non-reflective and may represent a layer of heterolithic and/or hydrothermally altered material erupted from this crater. In contrast to the subaerial craters, which have radial aprons of explosion breccia deposits that rim the crater (Hamilton, 1987; Muffler et al., 1971), many of the sublacustrine circular depressions lack an obvious apron. This may indicate either more widespread dispersal of ejection deposits in the lake water or that some other process, such as catastrophic collapse of sealed cap rock, created the depressions.

Following the initial major explosive event of Elliott's Crater, lacustrine sediments, imaged as laminated reflective layers in the seismic profile (Fig. 3B), accumulated in the floor of the crater and on its south flank. Post-eruptive sediment thickness of $\sim 8$ m indicates the main hydrothermal explosion occurred between 8 and 13 ka, based on sedimentation rates in the lake. Opaque zones within the stratified sedimentary fill of the crater indicate the presence of hydrothermal fluids and/or gases. The presence of two younger craters at the south end of the main crater floor further indicates more recent hydrothermal activity and possibly younger explosions. A north–south seismic profile across Elliott's explosion crater shows about 10 m of vertical difference in height between the rims. This difference may result from doming associated with hydrothermal activity prior to initial explosion.

### 3.4. Hydrothermal vents on the floor of Yellowstone Lake

Seismic reflection profiles of the surveyed areas in the northern and West Thumb basins of Yellowstone Lake reveal a lake floor covered with laminated diatomaceous lacustrine muds, many of which are deformed, disturbed, and altered. High-resolution bathymetric mapping reveals that many areas contain small ($< 20$ m) depressions pockmarking the lake bottom (Fig. 2). In seismic reflection profiles (Fig. 3B), these features typically are imaged as V-shaped structures associated with reflective layers that are deformed or have sediments draped across their edges. Areas of high opacity or no reflection occur directly beneath them and are interpreted as gas pockets, gas-charged fluids, or hydrothermally altered zones. Evidence for lateral movement of hydrothermal fluids is seen beneath and adjacent to hydrothermal vents identified in the seismic reflection profiles. The areas of opacity in the seismic data and of low values of magnetic intensity in the aeromagnetic data represent larger zones of hydrothermal alteration than seen in the surficial hydrothermal vents (Finn and Morgan, 2002).

Many vent areas are associated with smaller domal structures in which the laminated diatomaceous lacustrine sediments have been domed upward as much as several meters by underlying pockets of gas or gas-charged fluids, presumably rich in steam and possibly $CO_2$. Hydrothermal activity beneath the domes silicifies the sediments causing them to become sealed, impermeable, and weakly lithified so that their resultant compaction is minimal. The unaltered zones of muds surrounding these domes become more compacted over time and contribute to the overall domal morphology. These domal structures may be precursors to small hydrothermal explosions, collapse zones, and areas where active hydrothermal venting may develop in the future.

Our seismic reflection studies clearly identify sublacustrine hydrothermal vents with associated hydrothermal feeders. Much of the deformation and alteration can be attributed to hydrothermal vent channelways, subsurface migration, and ascent of hydrothermal fluids. In contrast, areas devoid of inferred hydrothermal vents show well-laminated seismic reflections characteristic of lake sediments. Over 150 vents have been mapped in the northern basin. Several thermal fields also are identified in West Thumb basin, including a large northeast-trending one in the southeast, another in the northwest, and several in the west (Fig. 2B). These fields contain dozens of small hydrothermal vents in various stages of development and activity.

### 3.5. Siliceous spires

Siliceous spires in Bridge Bay (Fig. 2C) in the northern basin of Yellowstone Lake were discovered in 1997 and are described here because they represent an end-member of hydrothermal deposit development in the lake clearly imaged by multibeam sonar studies. Approximately 12–15 spires are identified in water depths of 15 m. These roughly conical structures (Fig. 4A) are up to 8 m in height and up to 10 m wide at the base. A small 1.4-m-tall spire collected from Bridge Bay in cooperation with the National Park Service in 1999 shows the spire base to be shallow ($\sim$0.5 m below the sediment–water interface), irregular, and rounded; spire material above the sediment–water interface constitutes about 75% of the entire structure.

The sediment–water interface or the lake floor is recorded on the spire as a zone of banded ferromanganese oxide-stained clay-rich and diatomaceous sediments. Below the sediment–water interface, the spire is not oxidized whereas above it, the spire has a dark reddish-brown oxide coating (Fig. 4B). The interior of the collected spire is white, finely porous, and has thin (from 0.3 to $<$3 cm diameter), anastomozing vertical channels through which hydrothermal fluids flowed. Little oxide occurs in the interior of the spire structure, but oxidation surfaces are present on former growth fronts (Fig. 4B).

Chemical and oxygen isotope analyses and scanning electron microscope (SEM) studies of spire samples show them to be composed of silicified bacteria, diatom tests, and amorphous silica produced by sublacustrine hydrothermal vent processes (Fig. 4C). Geochemical studies of lake waters, hydrothermal vent fluids, and waters in tributary streams show that Yellowstone Lake waters and vent fluids are enriched in As, Mo, Tl, Sb, and W (Balistrieri et al., 2003). Similarly, the Bridge Bay spires are strongly enriched in As, Ba, Mn, Mo, Tl, Sb, and W (Fig. 4D). Oxygen isotopic values suggest formation of the spires at about 70–90°C. U-series disequilibrium dating of two samples from one spire yields dates of about 11 ka (ages were determined by Neil Sturchio, written communication, 1998); thus, the spire analyzed is immediately post-glacial. Spires may be analogous in formation to black-smoker chimneys, well-documented hydrothermal features associated with deep-seated hydrothermal processes at oceanic plate boundaries that precipitate on the seafloor due to mixing between hydrothermal fluids and cold bottom waters (Tivey, 1995).

### 3.6. Fissures and faults

Features identified in the western area of the northern and central basins (Fig. 2A,C,D) include a set of sub-parallel, elongate, north-northeast-trending fissures west of Stevenson Island extending southward toward Dot Island (Fig. 2A); a series of en echelon, linear, northwest-trending, fissure-controlled, small depressions east and southeast of Stevenson Island; and a graben north of Stevenson Island, nearly on strike with Lake Village (Fig. 1B).

The sub-parallel fissures west of Stevenson Island (Fig. 2A,C) cut as much as 10–20 m into the soft-sediment lake floor 0.5 km southeast of Sand Point. These fissures represent extension fractures whose orientation is controlled by regional north–south structural trends, recognized both north and south of Yellowstone Lake. Active hydrothermal activity is localized along the fissures as shown by dark oxide precipitates and warm shimmering fluids upwelling from them. The fissures, inspected with the submersible ROV for about 160 m along their NNE trend are narrow ($<$2 m wide) and cut vertically into soft laminated sediments. No vertical or strike-slip displacement is observed. A parallel set of N–S-trending fissures also occurs 1.3 km northeast of Sand Point (Fig. 2C). Farther south along this trend, the fissures appear to have well-developed hydrothermal vent craters, although investigations with the submersible show only weak or inactive vent fields in the central basin. Examination of the high-resolution magnetic intensity map of this area shows a linear zone of relatively lower magnetic intensities that spatially coincides with the fissures and graben (Figs. 1C and 2B,D).

Observation of the features east of Stevenson Island (Fig. 2C) using the submersible ROV indicates that small, well-developed hydrothermal vents coalesce along northwest-trending fissures. These may be similar to, but more developed, than those west of Stevenson Island. A large hydrothermal vent at the south end of the northernmost set of aligned vents, in the deepest part of Yellowstone Lake, at 133 m, emits hydrothermal fluids as hot as 120°C.

Finally, east–west seismic reflection profiles across the down-dropped block north of Stevenson Island reveal a north-northwest-trending graben structure bounded by normal faults. This graben was identified by previous investigations (Kaplinski, 1991; Otis et al., 1977; Shuey et al., 1977) but our studies, using differential GPS navigation and high-resolution seismic and bathymetric data, provide the first accurate information on location and displacement on this important structure. Measured displacements along the two bounding faults are variable, but displacement along the western boundary is generally $\sim$6 m whereas that along the eastern normal fault is $\sim$2 m. The eastern bounding fault cuts Holocene lake sediments, indicating recent movement. Seismic profiles across the graben indicate the graben projects (or strikes) toward Lake Village (Figs. 1B and 2C), posing a potential seismic hazard in that area.

The sublacustrine fissures and faults revealed by the high-resolution bathymetry are related to the regional tectonic framework of the northern Rocky Mountains, variable depths to the brittle–ductile transition zone (Fournier, 2000), and the subcaldera magma chamber (Eaton, 1975; Fournier, 1989; Fournier et al., 1976; Lehman et al., 1982; Stanley et al., 1991; Wicks et al., 1998) and play important roles in shaping the morphology of the floor of Yellowstone Lake. Many recently identified features along the western margin of the northern and central basins, such as the active fissures west of Stevenson Island and the active graben north of it, are oriented roughly north–south and may be related to a regional structural feature in western Yellowstone Lake on strike with the Neogene Eagle Bay fault zone (Fig. 1B) (Locke and Meyer, 1994; Pierce et al., 1997). Seismicity maps of the Yellowstone region (see U.S. Geological Survey Yellowstone Volcano Observatory website: http://volcanoes.usgs.gov/yvo) show concentrations of epicenters along linear N–S trends in the northwestern portion of the lake.

### 3.7. Landslide deposits

Multi-beam bathymetric data reveal hummocky lobate terrain at the base of slopes along the northeast and parts of the eastern margin of the lake basin (Fig. 2A). Seismic reflection data indicate that the deposits range in thickness from $\geq$10 m at the eastern edge of the lake and are recognizable as thin ($<$1 m) units extending up to 500 m into the interior of the lake basin. We interpret these as landslide deposits. The thickness of the lacustrine sediment cap deposited above the landslide deposits is variable and suggests that the landslides were generated by multiple events. We suggest the landslides were triggered by ground shaking associated with earthquakes and (or) hydrothermal explosions. The eastern shore of Yellowstone Lake, near where these landslide deposits occur, marks the margin of the Yellowstone caldera (Christiansen, 1984, 2001; Hildreth et al., 1984; U.S.G.S., 1972) and abuts steep terrain of the Absaroka Mountains to the east, both possible factors contributing to landslide events. The volume of material identified in these deposits would result in a significant displacement of water in the lake and may pose a potential hazard on shore.

### 3.8. Submerged shorelines

Several submerged former lake shorelines form underwater benches in the West Thumb and northern basins of Yellowstone Lake (Fig. 2A–C). The submerged, shallow margins (depth $<$15–20 m) of the northern basin are generally underlain by one to three relatively flat, discontinuous, post-glacial terraces that record the history of former lake levels. Correlation of these submerged shoreline terraces around the lake is based primarily on continuity inferred from multi-beam bathymetric data and shore-parallel seismic reflection profiles. These data indicate that lake levels were significantly lower in the past. An extensive bench occurs south of Steamboat Point and along the western shore of the northern basin south of Gull Point (Fig. 2C). In Bridge Bay, submerged beach pebbly sand 5.5 m below the present lake level yielded a carbon-14 date of

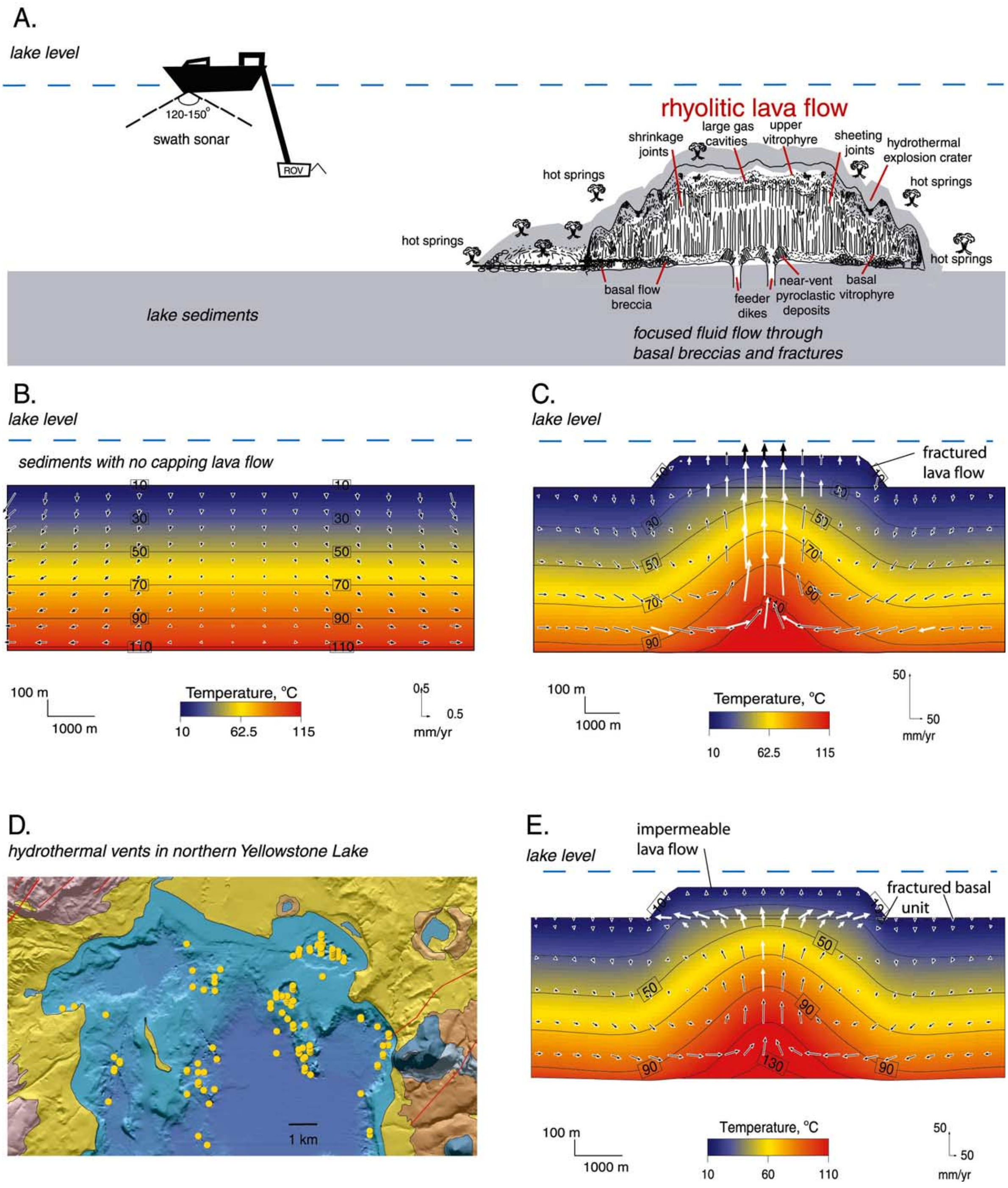
A.
lake level
120-150°
swath sonar
ROV
rhyolitic lava flow
shrinkage joints
large gas cavities
upper vitrophyre
sheeting joints
hydrothermal explosion crater
hot springs
hot springs
hot springs
hot springs
basal flow breccia
feeder dikes
near-vent pyroclastic deposits
basal vitrophyre
lake sediments
focused fluid flow through basal breccias and fractures
B.
lake level
sediments with no capping lava flow
10
30
50
70
90
110
100 m
1000 m
Temperature, °C
10
62.5
115
0.5
0.5
mm/yr
C.
lake level
fractured lava flow
10
30
50
70
90
110
100 m
1000 m
Temperature, °C
10
62.5
115
50
50
mm/yr
D.
hydrothermal vents in northern Yellowstone Lake
1 km
E.
lake level
impermeable lava flow
fractured basal unit
10
50
90
130
100 m
1000 m
Temperature, °C
10
60
110
50
50
mm/yr

3835 yr (Pierce et al., 2002). Well-developed submerged shoreline terraces are present in West Thumb basin, especially along its southern and northern edges.

Relief on these terraces is as much as 2–3 m, a measure of post-depositional vertical deformation. Documentation of the submerged terraces adds to a database of as many as nine separate emergent terraces around the lake (Locke and Meyer, 1994; Locke et al., 1992; Meyer, 1986; Pierce et al., 2002). Changes in lake level over the last 9500 radiocarbon years have occurred primarily in response to episodic uplift and subsidence (inflation and deflation) of the central part of the Yellowstone caldera (Dzurisin et al., 1994; Pelton and Smith, 1982; Pierce et al., 1997, 2002; Wicks et al., 1998). Holocene changes in lake level recorded by these terraces have been variably attributed to intra-caldera magmatic processes, hydrothermal processes, climate change, regional extension, and (or) glacioisostatic rebound (Dzurisin et al., 1994; Locke and Meyer, 1994; Meyer and Locke, 1986; Pierce et al., 1997, 2002; Wicks et al., 1998).

## 4. Discussion

### *4.1. Do the newly discovered features in Yellowstone Lake pose potential geologic hazards?*

The bathymetric, seismic, and submersible surveys of Yellowstone Lake reveal significant potential hazards exist on the lake floor. Hazards range from potential seismic activity along the western edge of the lake to hydrothermal explosions to landsliding associated with explosion and seismic events to sudden collapse of the lake floor through fragmentation of hydrothermally altered cap rocks. Any of these events could result in a sudden shift in lake level, generating large waves that could cause catastrophic local flooding. Deposits from these waves may be similar in character to what is now exposed along the wave-cut cliffs of Mary Bay. Here, dark, well-sorted, cross- to planar-bedded, generally fine-grained sands are present at the base of and within the Mary Bay explosion breccia deposit. These types of deposits are likely ephemeral and the likelihood of their preservation in the stratigraphic record is slight. The sand unit below the Mary Bay breccia is 1.5 to $>2$ m thick and contains numerous small en echelon faults. These deposits are similar to other paleoseismites (Bartholomew et al., 2002). We conclude that this sand unit represents a deposit from a possible earthquake-generated tsunami-like wave, which may be related to triggering the explosion of the Mary Bay crater complex (Morgan et al., 2002).

Ejecta from past hydrothermal explosions that formed craters in the floor of Yellowstone Lake extend several kilometers from their crater rims and include rock fragments in excess of several meters in diameter (Hamilton, 1987; Love et al., 2003; Morgan et al., 1998; Richmond, 1973, 1974, 1976, 1977). Deposits from the Indian Pond hydrothermal explosion event extend as much as 3 km from its crater and are as thick as 3–4 m

Fig. 5. (A) Schematic diagram showing physical features of a rhyolitic lava flow (modified from Bonnichsen and Kauffman, 1987). (B) Two-dimensional fluid flow model with simple glaciolacustrine sedimentary aquifer (no cap rock), which results in low flow velocities, recharge at the surface, and lateral flow out of both ends of the model aquifer. Subsurface temperatures never exceed 114°C, as indicated by contours and color map. Fluid flow rates are low ($<1$ mm/yr) as indicated by velocity vectors. (C) Fluid flow model with a fully cooled rhyolitic lava flow acting as cap rock. The underlying sedimentary aquifer and heat flow are exactly the same as in the previous model. The addition of a 190-m-thick fractured crystalline rock cap strongly focuses the upward limb of an intense convection cell under the cap rock. In this model, fluid temperatures reach 140°C, and flow velocities are as high as 150 mm/yr. (D) Locations of hydrothermal vents on the lake floor mapped using seismic reflection. Lava flow boundaries are based on high-resolution bathymetry and aeromagnetic data. (E) Fluid flow model that includes a basal breccia zone beneath an impermeable lava flow. The lower sedimentary unit is overlain by a thin fractured lava flow unit (20 m thick) that extends the entire width of the sedimentary prism. Above the more permeable basal unit is a 170-m-thick low-permeability unfractured lava flow. Flow vectors indicate strong upflow under the lava flow, with maximum subsurface temperatures of $\sim$150°C and flow rates up to 160 mm/yr. Upflow is deflected laterally within the 20-m-thick 'basal' fractured zone toward the flow edges, resulting in hydrothermal venting on the lake floor near the margins of lava flows.

(Pierce et al., 2002). In addition, the threat of another Mary Bay-sized explosion event may exist, as indicated by the abundance of hydrothermal venting and domal structures in the northern basin where heat flow values and temperatures are extremely high.

In addition to hazards affecting humans, hydrothermal explosions are likely to be associated with the rapid release into the lake of steam and hot water (Fournier et al., 1991), possibly affecting water chemistry by the release of potentially toxic trace metals. Such changes could have significant impact on the fragile ecosystem of Yellowstone Lake and vicinity (Shanks et al., 2001; Chaffee et al., 2003).

### 4.2. *Do rhyolitic lava flows control hydrothermal activity?*

One of the basic observations from our surveys is that a close spatial relationship exists between the distribution of hydrothermal vents, explosion craters, and sublacustrine rhyolitic lava flows. Does the presence of fully cooled lava flows in a subaqueous environment affect the distribution of hydrothermal vents? Could the identification of rhyolitic lava flows be used as a tool to help predict where some hydrothermal activity may occur in the future?

The floor of Yellowstone Lake, two-thirds of which is within the Yellowstone caldera, lies above a large magma chamber that may be periodically replenished (Eaton, 1975; Fournier, 1989; Fournier et al., 1976; Lehman et al., 1982; Stanley et al., 1991; Wicks et al., 1998). The relationship between sublacustrine hydrothermal features and the areas of high relief, interpreted here as rhyolitic lava flows, can be seen in Figs. 1B, 2A, and 5D. Based on our observations of the abundant present-day distribution of hydrothermal vents, we infer that fully cooled rhyolitic lava flows exert a fundamental influence on subsurface hydrology and hydrothermal vent locations. We speculate that upwelling hydrothermal fluids are focused preferentially through rhyolitic lava flows whereas hydrothermal fluids conducted through lake and glacial sediments tend to be more diffuse (Fig. 5). In addition, convective flow moves laterally away from thicker, more impermeable segments of the rhyolite flow toward the fractured flow margin, where the majority of hydrothermal activity is observed (Fig. 5E).

In order to evaluate the effect of rhyolitic lava flows on convective fluid flow in the sublacustrine environment, three simple two-dimensional flow models were constructed (Fig. 5). Flow modeling was carried out using the program Basin2, v. 4.0.1, 1982–1999, developed by Craig Bethke, University of Illinois. This program uses finite difference methods to solve Darcy's law for fluids of varying density. The program allows the user to model topographic, compaction-driven, and/or convective flow by setting parameters related to fluid density and viscosity, heat capacity, heat flow, porosity and permeability.

The first model involves fluid flow in a sediment volume 1 km thick by 10 km wide (Fig. 5B) covered by lake water 200 m deep. Both left and right edges of the sediment volume are open to flow. Closing left and right boundaries results in an almost stagnant flow situation, so that option was not pursued further. Vertical direction permeability ($z$) is $10^{-15}$ m$^2$, and horizontal direction ($x$) permeability is $10^{-14}$ m$^2$, properties expected for lacustrine or glacial sediments. In order to simulate a magma chamber at depth, heat flow through the base of the section is set at 4 HFU or 167.6 mW/m$^2$ (one heat flow unit = $10^{-6}$ cal/cm$^2$/s = 41.9 mW/m$^2$), much higher than a typical continental value of 40–70 mW/m$^2$. The basal heat flow value used in these calculations produces the highest possible thermal gradient without violating the assumptions of the modeling approach (boiling not allowed, fluid density and viscosity extremes not allowed, fluid temperature $< 300$°C). Results of this fluid flow model (Fig. 5B) indicate uniform increase of temperature with depth to a maximum of 114°C, recharge at the surface, flow out both ends, and low fluid flow rates of $< 1$ mm/yr.

Addition of a sublacustrine 190-m-thick cap rock, in this case a fully cooled lava flow, on top of the model sedimentary section (Fig. 5C) produces dramatic changes in fluid flow. The fractured lava flow is assigned permeabilities of

$2.5\times10^{-14}$ m$^2$ in the $z$-direction and $5\times10^{-14}$ m$^2$ in the $x$-direction, within the range measured for fractured volcanic rocks. Results indicate that a sublacustrine lava flow atop the sediment causes focusing of intense thermal upflow through the lava flow and strong discharge at the surface of the flow into the overlying lake waters. In contrast to the simple sedimentary model, fluid flow rates beneath the lava flow cap rock range up to 150 mm/yr and temperatures are $\geq 140°C$.

Our bathymetric mapping shows hydrothermal vents in the lake are concentrated along lava flow margins and structures such as the caldera margin and fissures in the northern and central basin. To simulate the effects of a lava flow with a thick impermeable cap that thins towards its margins and has a basal breccia zone, a three-layer model was applied. In this case, the lower sedimentary prism is unchanged but is overlain by a thin (20 m) basal unit with the properties of a fractured lava flow, which is capped by a 170-m-thick unfractured lava flow with low permeability. In this case, the unfractured portion of the lava flow is assigned permeabilities of $6.3\times10^{-16}$ m$^2$ in the $z$-direction and $6.3\times10^{-15}$ m$^2$ in the $x$-direction, within the range measured for unfractured volcanic rocks.

Results of this model (Fig. 5E) indicate strong convective upflow under the lava flow, with maximum subsurface temperatures of 150°C and flow rates up to 160 mm/yr. As expected, upflow is strongly influenced by the overlying low-permeability unfractured lava flow and is deflected laterally to the edges of the flow. Lateral flow proceeds within the 20-m-thick 'basal' fractured zone away from the central upwelling zone toward the flow edges on either side, resulting in hydrothermal venting on the lake floor near the margins of lava flows. This physical model explains the preferential distribution of hydrothermal vents located near or at the edges of rhyolitic lava flows in Yellowstone Lake (Fig. 5D).

## 5. Summary and conclusions

Mapping in Yellowstone Lake extends subaerial geologic mapping, allowing the lake basin to be understood in the geologic context of the rest of the Yellowstone region (Blank, 1974; Christiansen, 1974, 2001; Richmond, 1973; U.S.G.S., 1972). Rhyolitic lava flows contribute greatly to the geology and morphology of Yellowstone Lake, as they do to the subaerial morphology of the Yellowstone Plateau. We infer from our high-resolution bathymetry and aeromagnetic data that Stevenson, Dot, and Frank Islands are underlain by large-volume rhyolitic lava flows (Fig. 2A). Mapped late Pleistocene glaciolacustrine sediment deposits on these islands merely mantle or blanket the flows (Otis et al., 1977; Richmond, 1974; Richmond and Waldrop, 1975; Shuey et al., 1977). Similarly, the hydrothermally cemented beach deposits exposed on Pelican Roost, located ~1 km southwest of Steamboat Point (Fig. 2C), blanket another submerged large-volume rhyolite flow. The margin of the Yellowstone caldera (Otis et al., 1977; Richmond, 1974; Richmond and Waldrop, 1975; Shuey et al., 1977) passes through the central part of the lake and northward along the lake's eastern edge (Fig. 1). Similar to most of the rest of the topographic margin of the Yellowstone caldera (Fig. 1A), we suggest that post-collapse rhyolitic lava flows are present along much of the caldera margin beneath Yellowstone Lake and control much of the distribution of the sublacustrine hydrothermal vents. Many potential hazards have been identified in our mapping effort. Next steps will include hazard assessments and methodologies to be employed in monitoring these potentially dangerous features under the aegis of the Yellowstone Volcano Observatory.

**Acknowledgements**

We thank Kate Johnson, Ed duBray, Geoff Plumlee, Pat Leahy, Steve Bohlen, Tom Casadevall, Linda Gundersen, Denny Fenn, Elliott Spiker, Dick Jachowski, Mike Finley, John Varley, Tom Olliff, and Paul Doss for supporting this work. We thank Dan Reinhart, Lloyd Kortge, Paul Doss, Rick Fey, John Lounsbury, Ann Deutch, Jeff Alt, Julie Friedman, Brenda Beitler, Charles Ginsburg, Pam Gemery, Rick Sanzolone, Dave Hill, Bree Burdick, Eric White, Jim Bruckner, Jim Waples, Bob Evanoff, Wes Miles, Rick Mossman, Gary Nelson, Christie Hendrix, and Tim Morzel and many others for assistance with field studies. We thank Neil Sturchio for preliminary uranium-series dating of spire samples. We thank Patrick Browne, Bryan Davey, Bob Christiansen, Karl Kellogg, Geoff Plumlee, Patrick Muffler, and Shaul Hurwitz for constructive reviews that substantially improved the manuscript. We are grateful to Coleen Chaney, Debi Dale, Joan Luce, Mary Miller, Sandie Williamson, Vicky Stricker, and Robert Valdez for their skillful assistance with project logistics. This research was supported by the U.S. Geological Survey, the National Park Service, and the Yellowstone Foundation.

## References

Balistrieri, L.S., Shanks, W.C. III, Cuhel, R.L., Aguilar, C., Klump, J.V., 2003. The influence of sublacustrine hydrothermal vents on the geochemistry of Yellowstone Lake. In: Morgan, L.A. (Ed.), Integrated Geoscience Studies in the Greater Yellowstone Area: Volcanic, Hydrothermal, and Tectonic Processes in the Yellowstone Geoecosystem. U.S. Geological Survey Professional Paper (in press).

Bartholomew, M.J., Stickney, M.C., Wilde, E.M., Dundas, R.G., 2002. Late Quaternary paleoseismites: Syndepositional features and section restoration used to indicate paleoseismicity and stress-field orientations during faulting along the main Lima Reservoir fault, southwestern Montana. In: Ettensohn, F.R., Rast, N., Brett, C.E. (Eds.), Ancient Seismites. Geological Society of America Special Paper 359, pp. 29–48.

Blank, H.R., 1974. Geologic map of the Frank Island quadrangle, Yellowstone National Park, Wyoming. U.S. Geological Survey, Geological Quadrangle Map, GQ-1209a, Scale 1:62,500.

Bonnichsen, B., Kauffman, D.F., 1987. Physical features of rhyolite lava flows in the Snake River plain volcanic province, southwestern Idaho. In: Fink, J.H. (Ed.), The Emplacement of Silicic Domes and Lava Flows. Geological Society of America Special Paper 212, Boulder, CO, pp. 119–145.

Browne, P.R.L., Lawless, J.V., 2001. Characteristics of hydrothermal eruptions, with examples from New Zealand and elsewhere. Earth-Sci. Rev. 52, 299–331.

Chaffee, M.A. et al., 2003. Applications of trace-element and stable-isotope geochemistry to wildlife issues, Yellowstone National Park and vicinity. In: Morgan, L.A. (Ed.), Integrated Geoscience Studies in the Greater Yellowstone Area: Volcanic, Hydrothermal, and Tectonic Processes in the Yellowstone Geoecosystem. U.S. Geological Survey Professional Paper (in press).

Christiansen, R.L., 1974. Geologic map of the West Thumb Quadrangle, Yellowstone National Park, Wyoming. U.S. Geological Survey, Geological Quadrangle Map, GQ-1191, Scale 1:62,500.

Christiansen, R.L., 1984. Yellowstone magmatic evolution: Its bearing on understanding large-volume explosive volcanism. In: Explosive Volcanism: Inception, Evolution, and Hazards. National Academy Press, pp. 84–95.

Christiansen, R.L., 2001. The Quaternary and Pliocene Yellowstone Plateau Volcanic Field of Wyoming, Idaho, and Montana. U.S. Geological Survey Professional Paper, 729-G, 145 pp.

Christiansen, R.L., Blank, H.R. Jr., 1975. Geologic map of the Canyon Village Quadrangle, Yellowstone National Park, Wyoming. U.S. Geological Survey, Geological Quadrangle Map, GQ-1192, Scale 1:62,500.

Dzurisin, D., Yamashita, K.M., Kleinman, J.W., 1994. Mechanisms of crustal uplift and subsidence at the Yellowstone Caldera, Wyoming. Bull. Volcanol. 56, 261–270.

Eaton, G.P. et al., 1975. Magma Beneath Yellowstone National Park. Science 188, 787–796.

Finn, C.A., Morgan, L.A., 2002. High-resolution aeromagnetic mapping of volcanic terrain, Yellowstone National Park. J. Volcanol. Geotherm. Res. 115, 207–231.

Fournier, R.O., 1989. Geochemistry and dynamics of the Yellowstone National Park hydrothermal system. Annu. Rev. Earth Planet. Sci. 17, 13–53.

Fournier, R.O., 2000. Hydrothermal processes related to movement of fluid from plastic into brittle rock in the magmatic-epithermal environment. Econ. Geol. 94, 1193–1212.

Fournier, R.O., Thompson, J.M., Cunningham, C.G., Hutchinson, R.A., 1991. Conditions leading to a recent small hydrothermal explosion at Yellowstone National Park. Geol. Soc. Am. Bull. 103, 1114–1120.

Fournier, R.O., White, D.E., Truesdell, A.H., 1976. Convective heat flow in Yellowstone National Park, Proceedings Second U.N. Symposium on the Development and Use of Geothermal Resources. U.S. Government Printing Office, Washington, DC, pp. 731–739.

Hamilton, W.L., 1987. Water level records used to evaluate deformation within the Yellowstone Caldera, Yellowstone National Park. J. Volcanol. Geotherm. Res. 31, 205–215.

Hildreth, W., Christiansen, R.L., O'Neil, J.R., 1984. Catastrophic isotopic modification of rhyolitic magma at times of caldera subsidence, Yellowstone Plateau volcanic field. J. Geophys. Res. 89, 8339–8369.

Kaplinski, M.A., 1991. Geomorphology and geology of Yellowstone Lake, Yellowstone National Park, Wyoming. M.Sc. Thesis, Northern Arizona University, Flagstaff, AZ, 82 pp.

Klump, J.V., Remsen, C.C., Kaster, J.L., 1988. The presence and potential impact of geothermal activity on the chemistry and biology of Yellowstone Lake, Wyoming. In: DeLuca, M., Babb, I. (Eds.), Global Venting, Midwater and Benthic

Ecological Processes. NOAA Symposium on Undersea Research, NOAA, pp. 81–98.

Lehman, J.A., Smith, R.B., Schilly, M.M., 1982. Upper crustal structure of the Yellowstone caldera from seismic delay time analyses and gravity correlations. J. Geophys. Res. 87, 2713–2730.

Locke, W.W., Meyer, G.A., 1994. A 12,000-year record of vertical deformation across the Yellowstone caldera margin: The shorelines of Yellowstone Lake. J. Geophys. Res. 99, 20079–20094.

Locke, W.W., Meyer, G.A., Pings, J.C., 1992. Morphology of a postglacial fault scarp across the Yellowstone (Wyoming) caldera margin, United States, and its implications. Bull. Seismol. Soc. Am. 82, 511–516.

Love, J.D., Good, J.M., Brown, D., 2003. Lithology, fossils, and tectonic significance of Pleistocene lake deposits in and near ancestral Yellowstone Lake. In: Morgan, L.A. (Ed.), Integrated Geoscience Studies in the Greater Yellowstone Area: Volcanic, Hydrothermal, and Tectonic Processes in the Yellowstone Geoecosystem. U.S. Geological Survey Professional Paper (in press).

Merrill, M.D., 1999. Yellowstone and the Great West: Journals, Letters, and Images from the 1871 Hayden Expedition. University of Nebraska Press, 315 pp.

Meyer, G.A., 1986. Genesis and deformation of Holocene shoreline terraces, Yellowstone Lake, Wyoming. M.Sc. Thesis, Montana State University, 94 pp.

Meyer, G.A., Locke, W.W., 1986. Origin and deformation of Holocene shoreline terraces, Yellowstone Lake, Wyoming. Geology 14, 699–702.

Morgan, L.A., Shanks, W.C., Pierce, K.L., Rye, R.O., 1998. Hydrothermal explosion deposits in Yellowstone National Park: Links to hydrothermal processes. EOS, Transactions, AGU fall annual meeting, 79, F964.

Morgan, L.A., Shanks, W.C. III, Pierce, K.L., 2002. Possible earthquake-generated wave deposits near Yellowstone Lake: Clues into triggering mechanisms of a large hydrothermal explosion crater. EOS, Transactions, AGU fall annual meeting.

Morgan, P., Blackwell, D.D., Spafford, R.E., Smith, R.B., 1977. Heat flow measurements in Yellowstone Lake and the thermal structure of the Yellowstone caldera. J. Geophys. Res. 82, 3719–3732.

Muffler, L.J.P., White, D.E., Truesdell, A.H., 1971. Hydrothermal explosion craters in Yellowstone National Park. Geol. Soc. Am. Bull. 82, 723–740.

Otis, R.M., Smith, R.B., Wold, R.J., 1977. Geophysical surveys of Yellowstone Lake, Wyoming. J. Geophys. Res. 82, 3705–3717.

Pelton, J.R., Smith, R.B., 1982. Contemporary vertical surface displacements in Yellowstone National Park. J. Geophys. Res. 87, 2745–2751.

Pierce, K.L., 1974. Surficial geologic map of the Tower Junction quadrangle and part of the Mount Wallace quadrangle, Yellowstone National Park, Wyoming and Montana. U.S. Geological Survey, Miscellaneous Geologic Investigations Map I-647, Scale 1:62,500.

Pierce, K.L., 1979. History and dynamics of glaciation in the northern Yellowstone National Park area. U.S. Geological Survey Professional Paper, 729-F, 89 pp.

Pierce, K.L., Cannon, K.P., Meyer, G., 1997. Yellowstone Caldera 'heavy breathing' based on Yellowstone Lake and River changes in post-glacial time. EOS Trans. Am. Geophys. Union 78, 802.

Pierce, K.L., Cannon, K.P., Meyer, G.A., Trebesch, M.J., Watts, R., 2002. Post-glacial inflation–deflation cycles, tilting, and faulting in the Yellowstone caldera based on Yellowstone Lake shorelines, U.S. Geological Survey Open-File Report 02-142, 65 pp.

Remsen, C.C. et al., 1990. Hydrothermal springs and gas fumaroles in Yellowstone Lake, Yellowstone National Park, Wyoming. Natl. Geogr. Res. 6, 509–515.

Richmond, G.M., 1973. Surficial geologic map of the West Thumb quadrangle, Yellowstone National Park, Wyoming. U.S. Geological Survey, Miscellaneous Geologic Investigations Map I-643, Scale 1:62,500.

Richmond, G.M., 1974. Surficial geologic map of the Frank Island Quadrangle, Yellowstone National Park, Wyoming. U.S. Geological Survey, Miscellaneous Geologic Investigations Map I-0642, Scale 1:62,500.

Richmond, G.M., 1976. Surficial geologic history of the Canyon Village Quadrangle, Yellowstone National Park, Wyoming, for use with map I-652. U.S. Geological Survey Bulletin B-1427, 35 pp.

Richmond, G.M., 1977. Surficial geologic map of the Canyon Village Quadrangle, Yellowstone National Park, Wyoming. U.S. Geological Survey, Miscellaneous Geologic Investigations Map I-652, Scale 1:62,500.

Richmond, G.M., Waldrop, H.A., 1975. Surficial geologic map of the Norris Junction quadrangle, Yellowstone National Park, Wyoming. U.S. Geological Survey, Miscellaneous Geologic Investigations Map I-650, Scale 1:62,500.

Shanks, W.C. III, Alt, J., Morgan, L.A., 2003. Geochemistry of sublacustrine hydrothermal deposits in Yellowstone Lake: hydrothermal reactions, stable isotope systematics, sinter deposition and spire growth. In: Morgan, L.A. (Ed.), Integrated Geoscience Studies in the Greater Yellowstone Area: Volcanic, Hydrothermal, and Tectonic Processes in the Yellowstone Geoecosystem. U.S. Geological Survey Professional Paper (in press).

Shanks, W.C. III, Balistrieri, L., Alt, J., Morgan, L.A., Meeker, G., Rye, R.O., Sturchio, N., Lovalvo, D., Cuhel, R., Klump, V., 2001. Geochemical Studies of Hydrothermal Vents and Sublacustrine Siliceous Deposits in Yellowstone Lake, Agenda and Abstracts, Yellowstone Lake: Hotbed of Chaos or Reservoir of Resilience? October 8–10, 2001. 6th Biennial Scientific Conference on the Greater Yellowstone Ecosystem. National Park Service, Yellowstone National Park, pp. 35–36.

Shuey, R.T., Ugland, R.O., Smith, R.B., 1977. Magnetic properties and secular variation in cores from Yellowstone and Jackson Lakes, Wyoming. J. Geophys. Res. 82, 3739–3746.

Smith, R.B., 1991. Earthquake and geodetic surveillance of Yellowstone. Seismol. Res. Lett. 62, 27.

Stanley, W.D., Hoover, D.B., Sorey, M.L., Rodriguez, B.D., Heran, W.D., 1991. Electrical geophysical investigations in the Norris-Mammoth corridor, Yellowstone National Park, and the adjacent Corwin Springs Known Geothermal Resources Area. U.S. Geological Survey Water Resources Investigations, 91-4052, D1–D18.

Tivey, M.K., 1995. Modeling chimney growth and associated fluid flow at seafloor hydrothermal vent sites. In: Humphris, S.E., Zierenberg, R.A., Mullineaux, L.S. Thomson, R.E. (Eds.), Seafloor Hydrothermal Systems; Physical, Chemical, Biological, and Geological Interactions. American Geophysical Union Monograph 91, Washington, DC, pp. 158–177.

U.S.G.S., 1972. Geologic map of Yellowstone National Park. U.S. Geological Survey, Miscellaneous Geological Investigations Map I-711, Scale 1:125,000.

Wicks, C.W., Jr., Thatcher, W.R., Dzurisin, D., 1998. Migration of fluids beneath Yellowstone Caldera inferred from satellite radar interferometry. Science 282, 458–462.

Wold, R.J., Mayhew, M.A., Smith, R.B., 1977. Bathymetric and geophysical evidence for a hydrothermal explosion crater in Mary Bay, Yellowstone Lake, Wyoming. J. Geophys. Res. 82, 3733–3738.